Effects of foundation conditions on infiltration-induced water level rise in road embankment

Hirohiko Kusaka[1] and A. Takahashi[1]

[1] Department of Civil and Environmental Engineering, Tokyo Institute of Technology, 2-12-1-M1-3 Ookayama, Meguro-ku, Tokyo 152-8552, Japan.

ABSTRACT

Estimation of water level for the persistent situation or prior to earthquake is crucial for evaluation of seismic performance of road embankments. Numerical modeling studies and model experiments are conducted to investigate effects of conditions of foundation on the water level in the embankment. Variations of rainfall intensity, permeability and thickness of permeable foundation are considered. Parametric study and model experiments reveal that the thinner the foundation thickness or the smaller the foundation permeability, the higher the convergent water level and water rise velocity.

Keywords: infiltration; water level; road embankment; foundation

1 INTRODUCTION

Earthquake-induced damage of the road embankments in the past reveals that high water level in the embankment prior to earthquake is one of the reasons that have led to severe damage of the embankments (Fujioka et al. 2016; Tameshige et al. 2009). Therefore, it can be said that estimation of the water level in the embankment for the persistent situation or prior to earthquake is crucial for evaluation of seismic performance of embankments. Screening of embankments vulnerable to earthquake due to the high water level has been made mainly based on geological and geomorphological information. However, for detailed assessment, soil properties, such as permeability and water retention characteristics, and their spatial distribution should be also considered.

The authors have shown the impact of foundation conditions, especially the thickness of the permeable foundation, on water level rise in the embankment through transient unsaturated seepage analysis (Kusaka and Takahashi 2018). In this study, various combinations of permeability in the embankment and its foundation are also considered. Further, model experiments are conducted to confirm observation in the numerical study.

2 PARAMETRIC STUDY BY SEEPAGE ANALYSIS

First, continuous rainfall-induced change of the water level in the embankment is calculated by two-dimensional saturated-unsaturated transient finite element seepage analysis. The program developed by authors is used. And the van Genuchten-Mualem prediction method (van Genuchten 1980) is employed to derive the soil-water characteristic curve and the relative coefficient of permeability. The SWCC used for the analysis is shown in Fig. 1. It is determined in reference to the tests on soils obtained from actual expressway embankments at Hokota, Ibaraki, Japan.

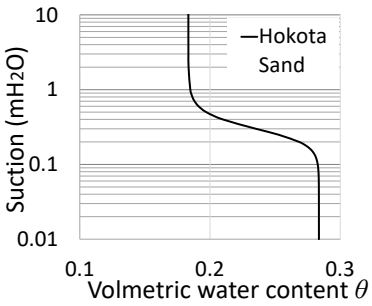

Fig. 1. SWCC used for numerical analysis.

The target embankment together with the boundary conditions is shown in Fig. 2 In the transient seepage analysis, the embankment surface is subjected to constant infiltration of rainwater throughout the analysis. The initial condition of the transient seepage analysis is obtained by the steady-state seepage analysis by setting the water table at the ground surface without rainfall. The authors have conducted the analysis by changing the shape of the embankment and foundation (Kusaka and Takahashi 2018). In this study, the authors change the permeability of the embankment and permeable foundation in the analysis.

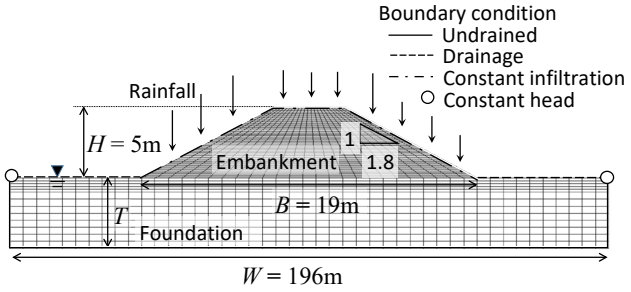

Fig. 2. Target embankment for numerical analysis.

Figure 3 is an example of the water level change in the embankment. The water level beings to rise after a certain period of time from the start of rainwater infiltration, and the rise converges at a certain level.

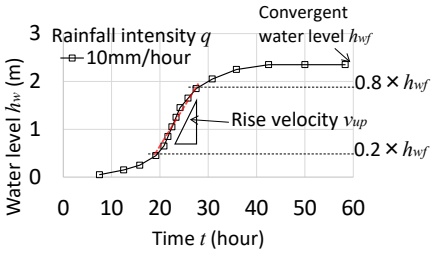

Fig. 3. Time-change of embankment water level

Figure 4 shows the relations between the convergent water level h_{wf} and the rainfall intensity normalized by saturated coefficient of permeability of embankment (hereinafter called "specific rainfall intensity q/k_{bsat}"). In Fig. 4, the results obtained by changing the thickness T and the coefficient of permeability of foundation k_{fsat} are plotted. As shown in the figure, the convergent water level rises linearly as the specific rainfall increases. In addition, as the foundation thickness and permeability decreases, the convergent water level rises.

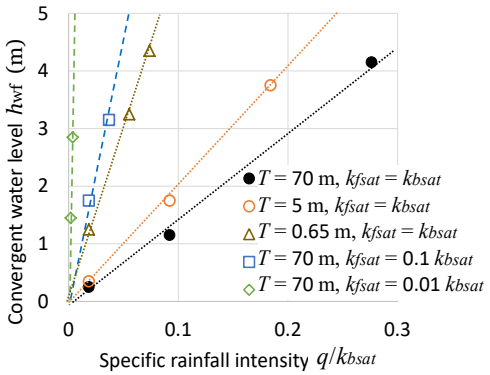

Fig.4. Convergent water level versus specific rainfall intensity.

Figure 5 shows the relations between specific rainfall intensity and water rise velocity normalized by saturated coefficient of permeability of embankment (hereinafter called "specific water rise velocity v_{up}/k_{bsat}"). The water rise velocity increases in proportion to the square of the rainfall intensity. In addition, as the foundation becomes thinner or the permeability of the foundation lowers, the water rise velocity increases.

From these results, we have confirmed that the water-level rises faster, and the convergent water level becomes high when drainage capacity of the foundation is low, e.g., thickness is small and/or permeability is low.

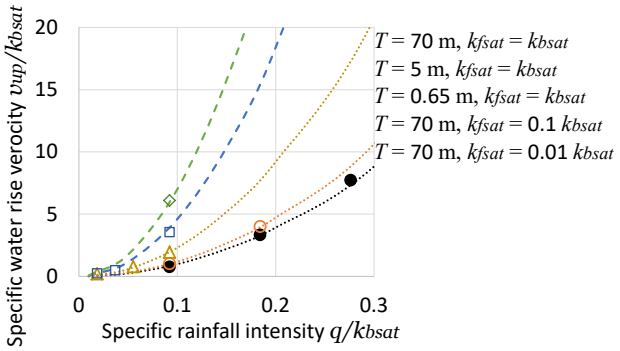

Fig.5. Specific water rise velocity versus specific rainfall intensity.

3 OUTLINE AND PROCEDURE OF MODEL EXPERIMENTS

Model tests are carried out to confirm the observation in the numerical study. Figure 6 is a schema of the model setup. The model simulates the center of embankment. The device at the top is the rain simulator, the soil column and base foundation model the embankment, and its foundation, respectively. In the soil column, soil moisture sensors and pore pressure transducers are installed to identify the water level. The bottom of rain simulator is composed by compacted soil, and water is filled over this soil. The amount of rainwater can be controlled by changing the water level of the rain simulator. *Edosaki* sand is used for the testing. The soil particle density is 2.7g/cm^3. The test cases and their test conditions are described in Fig. 6. Case 2 is used as a benchmark. The height of the column of Case 1 is bigger than Case 2; the thickness of the foundation of Case 3 is smaller than Case 2; the permeability of foundation of Case 4 is smaller than Case2.

The procedure of the experiments is as follows. First, the foundation and soil column are created with the prescribed dry density. Then, water is poured from the rain simulator into the column for saturation. Then poured water is stopped and drained from the bottom until the measured values converge and reach an equilibrium. The state of the soil column at convergence is set as the initial state. Next, a set amount of water is supplied continuously from the rain simulator, and the changes in the water content and pore water pressure when water infiltrate and water level is rising are measured.

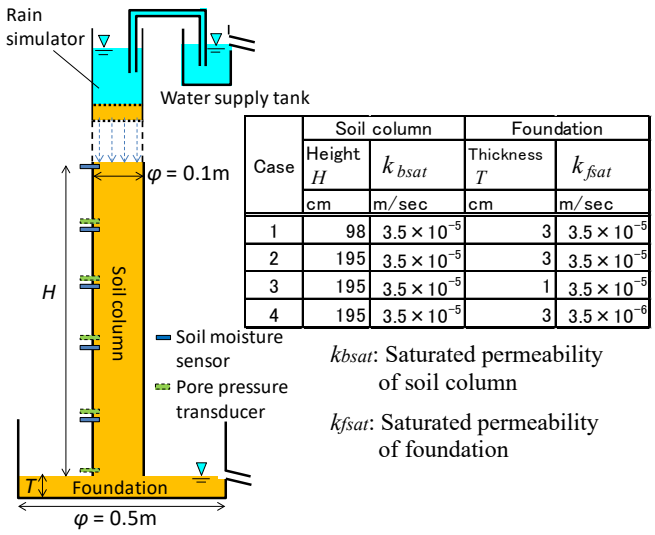

Case	Soil column		Foundation	
	Height H	k_{bsat}	Thickness T	k_{fsat}
	cm	m/sec	cm	m/sec
1	98	3.5×10^{-5}	3	3.5×10^{-5}
2	195	3.5×10^{-5}	3	3.5×10^{-5}
3	195	3.5×10^{-5}	1	3.5×10^{-5}
4	195	3.5×10^{-5}	3	3.5×10^{-6}

kbsat: Saturated permeability of soil column

kfsat: Saturated permeability of foundation

Fig.6. Experimental apparatus and test conditions.

4 TEST RESULTS

Figure 7 shows time histories of volumetric water content and pore water pressure for Case 4, when the rainfall intensity is 1.8×10^{-5} m/sec. The time rainfall started is set at 0 min. From 0 min to 200 min, the volumetric water content begins to rise in order starting from the top soil moisture sensor, meaning that infiltration progresses from top to bottom. When looking at soil moisture sensors installed at heights 76 cm and 116 cm, the volumetric water content converges temporarily, and then, the values start to rise in order from the bottom soil moisture sensor and up. This means that after infiltrated water reaches bottom, the water level begins to rise, and saturation of the soil column progresses gradually from the bottom and up. When looking at the soil moisture sensor at height 155 cm, the soil moisture level rose again slightly, but the volumetric water content converges at a lower value than that of the lower parts. And therefore, we can assume that the sand has not saturated at 155 cm and that the convergent water level is somewhere between 116 cm and 155 cm.

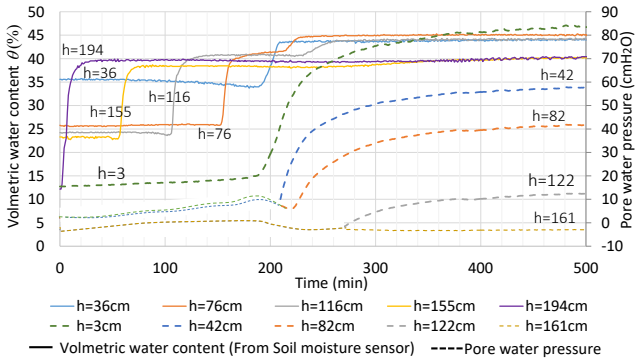

Fig.7. Time histories of volumetric water content and pore water pressure for Case 4 ($q = 1.8\times10^{-5}$m/sec.)

Figure 8 plots the infiltration speed against the rainfall intensity for each case. From Fig. 7, we can identify the time the volumetric water content begins to rise at each height. These times are set as the arrival time of the infiltration front from the top, and the infiltration speed is calculated from this time and the infiltration depth. The infiltration speed increases as rainfall intensity rises. From the fact that all the results are plotted approximately on the same curve, we can confirm that the permeability of the model soil column is the same for all the cases. We can also confirm that the thickness or the permeability of the foundation does not much affect the infiltration speed when the soil column is wetted from the top.

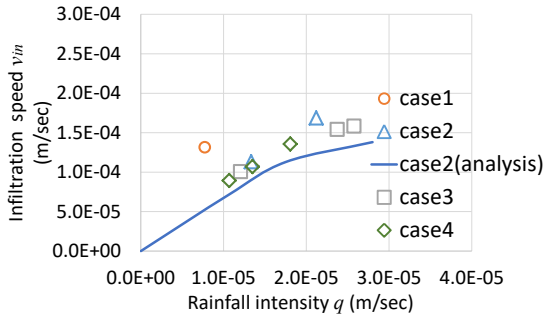

Fig.8. Infiltration speed versus rainfall intensity.

From Fig. 7, we can identify the time the volumetric water content converged to a saturation value and the time when the pore water pressure began to rise. Using these information, the water rise velocity v_{up} is calculated. Figure 9 shows the relationship between water rise velocity and rainfall intensity for Case 4. For other cases, water level rise is confirmed only when the degree of saturation is considerably high within the unsaturated zone. And therefore, a definite convergence time could not be derived and a definite water rise speed could not be confirmed. From Fig. 9, it can be seen that the water level rise velocity increases as the amount of rainfall rises. Figure 9 also shows the results of a seepage analysis conducted under the same condition and the results show a like trend.

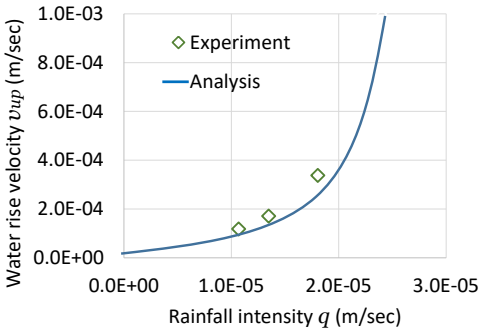

Fig.9. Water rise velocity versus rainfall intensity for Case 4.

Convergent water level h_{wf} can be estimated by distribution of the volumetric water content or pore water pressure. Figure 10 shows the relationship

between the convergent water level and rainfall intensity together with the results of the seepage analysis conducted under the same condition. From Fig. 10, as the rainfall intensity increases, the convergent water level rises. In Case 4, the convergent water level is higher than the other cases at the same rainfall intensity because the foundation permeability is low. This is confirmed by the numerical analysis. In contrast, when comparing Cases 2 and 3, which have different foundation thicknesses, we can see a difference in the numerical analysis, but there is no clear difference in the model test results. In this test, to confirm the effects of foundation thickness, we need to make the foundation thickness less than about 1cm to get a clear difference. That means we need to make a foundation with a thickness of several millimeters, and it could be that the foundation was not uniformly made with such precision.

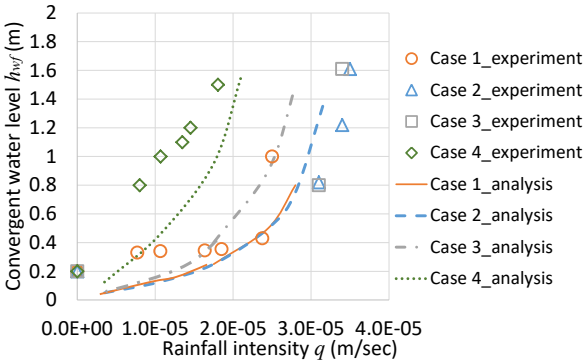

Fig.10. Convergent water level versus rainfall intensity.

Figure 11 shows the water level against the pore pressure at an elevation of 3cm from the base of the soil column in the tests together with the numerical analysis results. In general, the model tests and numerical simulations show similar tendency. At the same water level, the pore water pressure for Case 4 is higher than in other cases, and in Cases 1 to 3 the pore water pressure is considerably low compared with the hydrostatic value. This result indicates that even if the water level is the same, the pore water pressure differs greatly depending on the foundation condition. Furthermore, when focusing on the stability of embankment, Case 4 is less stable than the others because of the higher pore water pressure in the lower portion of the embankment.

5 CONCLUSION

In this study, Numerical modeling studies and model experiments are conducted to investigate effects of condition of foundation on the water level in the embankment. Variations of rainfall intensity, permeability and thickness of permeable foundation are

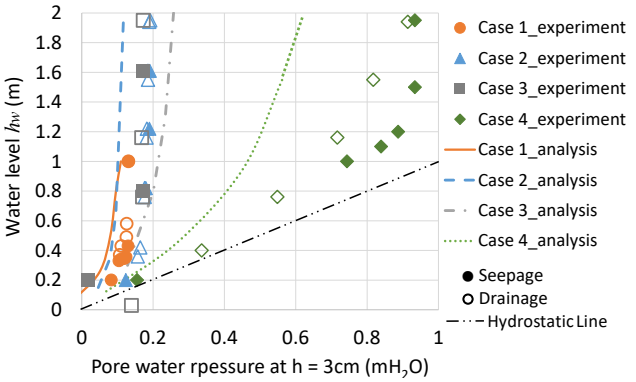

Fig.11. Water level versus pore water pressure of the base of the soil column.

considered. Parametric study and model experiments reveal that as the rainfall intensity rises the convergent water level and water rise velocity increases. In addition, the thinner the foundation thickness or the smaller the foundation permeability, the higher the convergent water level and rise velocity. From the test results, we have confirmed that when the permeability of the foundation is low, the pore water pressure in the lower portion of the embankment tends to be high even if the water level is the same. The fact indicates that, in the case with the lower permeability foundation, the strength of the soil in the lower portion of the embankment is smaller and hence the embankment is more instable.

Verification of the finding obtained from this study is planned by comparing with field measurements. Moreover, since layered foundation ground, anisotropy in permeability, evaporation and rainfall duration are not considered in this study, impacts of these should be examined in the future.

REFERENCES

Fujioka, K., Yokota, S., Kusaka., H. and Hirose, T. (2016). Analysis of Highway embankment for earthquake damage in the Tohoku district Pacific coast earthquake. Journal of Japan Association for Earthquake Engineering, 16(1), 285-308 (in Japanese).

Tameshige, M., Kawamura, K., Komada, S., Miyamura, M., Haibara, T. and Muroi, T. (2009). Noto Peninsula Earthquake damage to Noto Toll Road and its restoration -Embankment damage and countermeasure work. Japanese Geotechnical Journal, 4(4), 289-305 (in Japanese).

Kusaka, H., and Takahashi, A. (2018). Estimation of water level in road embankment by transient unsaturated seepage analysis. PanAm Unsaturated Soils 2017: Fundamentals, ASCE, GSP301, 175-184.

van Genuchten, M.T. (1980). A closed form equation for predicting the hydraulic conductivity of un-saturated soils. Journal of Soil Science Society of America, 44, 892-898.